^{19}F NMR studies of CaF_2 crystals doped with NdF_3, EuF_3, DyF_3, HoF_3, or TmF_3

Robert J. Booth* and Bruce R. McGarvey†
Department of Chemistry, University of Windsor, Windsor, Ontario N9B 3P4, Canada
(Received 24 August 1979)

^{19}F NMR at 46.6 MHz has been studied for single crystals of CaF_2 doped with NdF_3, DyF_3, HoF_3, and TmF_3 for doping concentrations of 0.5, 1.0, and 2.0 mol%. ^{19}F NMR at 84.67 MHz has been done for crystals doped with NdF_3 and EuF_3. Data on the main satellite lines, due to lattice fluorides having one nearest-neighbor rare-earth ion, show that the anisotropic portion of the NMR shift is entirely due to the direct dipolar interaction for all ions except Nd^{3+} and Eu^{3+}. Analysis of the isotropic portion of the shift and the nondipolar portion of the anisotropic shift reveals that the spin-transfer mechanism is primarily the polarization mechanism in the first half of the rare-earth series but that the covalent mechanism becomes predominant in the second half of the series. Evidence for extensive clustering is found in all systems studied in the form of resonance lines that must arise from lattice fluorides with two nearest-neighbor rare-earth ions. A possible form for the cluster is presented that will explain all the NMR results. T_1 measurements on the main ^{19}F line were done as a function of orientation for crystals doped with NdF_3 and EuF_3. In both cases, large variations with orientation were found. It is shown that present theories will account for this variation.

I. INTRODUCTION

Many optical, ESR, or electron-nuclear double resonance (ENDOR)[1] studies have been undertaken to determine the structure of defects and impurities in CaF_2 crystals doped with rare-earth trifluorides. Recently ^{19}F NMR studies have provided new information on these defects in CaF_2 (Refs. 2 and 3) and CdF_2 (Refs. 4 and 5). The earlier NMR studies dealt only with crystals doped with either ErF_3 or YbF_3. This work extends our earlier study[2] to crystals doped with NdF_3, EuF_3, HoF_3, DyF_3, and TmF_3.

CaF_2 has the fluorite structure which has a cubic lattice of fluoride ions with every other body-centered position occupied by a calcium ion. It has been established that the rare-earth ion substitutes for a calcium ion and the extra fluoride ion needed for electrical neutrality becomes an interstitial ion occupying one of the vacant body-centered sites. At low concentrations (< 0.05 mol%) there are found cubic sites for rare-earth ions in which the interstitial F^- ion is far removed from the rare-earth ion, tetragonal sites in which the interstitial F^- occupies the adjacent body-centered site, and to a less extent, trigonal sites in which the F^- interstitial is in the next-nearest vacant body-centered site.

Recent NMR studies[2,5] and laser studies[6] have shown that above 0.1 mol percent most of the rare-earth ions Yb^{3+} or Er^{3+} are found in clusters rather than the simple single ion sites found at lower concentrations. Evidence for at least pairwise clustering of Nd^{3+} was found by Kask and Kornienko[7] from the ESR spectrum of an interacting pair occupying nearest-neighbor sites along the [110] axis. Similar spectra for Tm^{2+} pairs was found by Baker and Marsh.[8] Little is known about the nature and structure of the clusters, and what is known is often contradictory. Cheetham and co-workers[9,10] have done neutron diffraction studies on CaF_2 doped with YF_3 and proposed two separate types of clusters depending on the concentration of dopant. Catlow[11] has attempted to calculate the formation energy of such clusters and was able to rationalize the neutron diffraction results. The NMR results[2,5] did not support these structures, however. An *ad hoc* "gettering" model has been advanced by Yaney *et al.*[12] to explain many of the diverse phenomena associated with formation of clusters at higher concentrations. In this model dimers and higher-order cluster "gettered" interstitial ions causing absolute concentration of tetragonal and trigonal sites to decrease with increasing doping concentration.

Our previous NMR studies[2] on CaF_2 containing 0.5, 1.0, and 2.0 mol% of ErF_3 or YbF_3 found resonances for lattice fluorides with one nearest-neighbor rare-earth ion. The crystals doped with YbF_3 also had a set of resonances that could be assigned only to a lattice fluoride with two nearest neighbor Yb^{3+} ions. Intensity measurements showed that most of the Yb^{3+} ions must be associated in dimers or higher-order clusters for the concentration studied. A third set of weaker lines was also found in YbF_3-doped crystals which must be due to a fluoride ion closely associated with two Yb^{3+} ions at normal nearest-neighbor distances, but the plane of the three ions must be canted to the (100) plane by $24° \pm 2°$. In ErF_3-doped crystals, two resonances were observed when the magnetic field was along the [100] axis that could not be lattice fluorides with one nearest neighbor of Er^{3+}. One was attributed to a lattice

fluoride with two nearest neighbors, while the second had an upfield shift so large that it could only be attributed to an interstitial fluoride with two nearest-neighbor Er^{3+} ions. This resonance was seen and more fully characterized in studies[5] on CdF_2 doped with ErF_3.

The previous studies analyzed the shifts for a fluoride with one rare-earth neighbor with the equation

$$\Delta B/B_0 = -[a_s + (a_p + a_m)(3\cos^2\theta - 1)], \quad (1)$$

where $\Delta B = B - B_0$ and B_0 is resonance field for the main line in the spectrum due to fluoride ions far removed from any rare-earth ion. The angle θ is the angle between the magnetic field and the vector connecting the rare-earth ion with the fluoride ion. The isotropic contribution from spin transfer is a_s which was found to be negative for both Er^{3+} and Yb^{3+}, while a_p is the corresponding contribution to the anisotropic portion of the shift. The direct dipolar contribution a_m from the rare-earth ion is given by

$$a_m = (\chi/R^3)\times 10^{-7}, \quad (2)$$

where χ is the magnetic susceptibility of the ion in S.I. (Systeme International) units and R is the interionic distance in m.

Experimentally it was found[2,4,5] that $a_p + a_m$ for Yb^{3+} and Er^{3+} is close to that calculated from Eq. (2) using the high-temperature limiting value for χ of

$$\chi = g_J^2 J(J+1)\mu_B^2/3kT, \quad (3)$$

where g_J is the Landé g factor for the given rare-earth ion, μ_B is the Bohr magneton, and the other symbols have their usual meaning. Thus for these ions a_p could be neglected. A theoretical calculation[13] of a_p for Yb^{3+} in CaF_2 found it to be ~20% of $a_p + a_m$.

II. EXPERIMENTAL

The cylindrical CaF_2 crystals doped with 0.5, 1.0, and 2.0 mol% LF_3 (L = Nd, Eu, Dy, Ho, and Tm) were supplied by Optovac, Inc., North Brookfield, Mass. They were 10 mm in diameter and 15 mm in length with the cylindrical axis being either the [100] or [110] axis. They were rigidly mounted at the end of a perspex rod which was mounted such that the cylindrical axis was perpendicular to the magnetic field. Using a 46.6-MHz spectrometer, the spectra were studied by rotating the magnetic field about this axis, while in the case of the 84.67-MHz spectrometer, the crystal was rotated instead.

Most of the NMR spectra were recorded using a broad-line spectrometer operating at 46.6 MHz which has been described elsewhere.[5,14] In addition, spectra for NdF_3- and EuF_3-doped crystals were obtained at 84.67 MHz with a Bruker CXP-100 high-power pulse spectrometer. It was not possible to observe the normal Fourier-transform (FT) spectrum with the Bruker CXP-100 because the 8-bit resolution of the high-speed digitizer prevented us from seeing the weak satellite lines in the presence of the intense main peak. We, therefore, eliminated most of the main peak by first applying an 180° pulse and then applying a measure pulse at the instance when the z magnetization was zero. The satellite peaks can be seen because T_1 for these lines is much shorter than that for the bulk fluorides far removed from the rare-earth ions. In order to get the rather large sweeps (1 MHz) needed to see all the satellite lines, the measure pulse was kept smaller than 10° and a magnitude calculation done in place of the usual phase correction routine normally used in FT spectra. This allowed for reasonable spectra even though B_1 was only ~1 mT. All spectra were done at room temperature (25 °C).

Relative line intensities for the broad-line spectra were made by numerical integration of the derivative curves obtained. When portions of the spectra required different gain settings, the settings were calibrated by comparing the intensity of the bulk fluoride resonance signal at both gain settings.

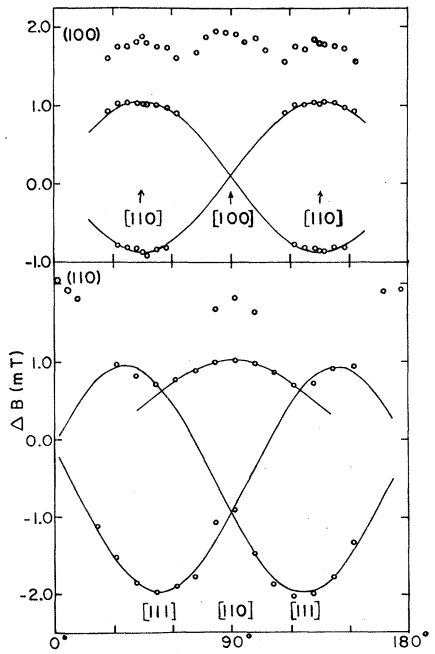

FIG. 1. Plot of line shifts vs angle between the [100] axis and the magnetic field for rotations in the (100) and (110) planes for $CaF_2(NdF_3)$.

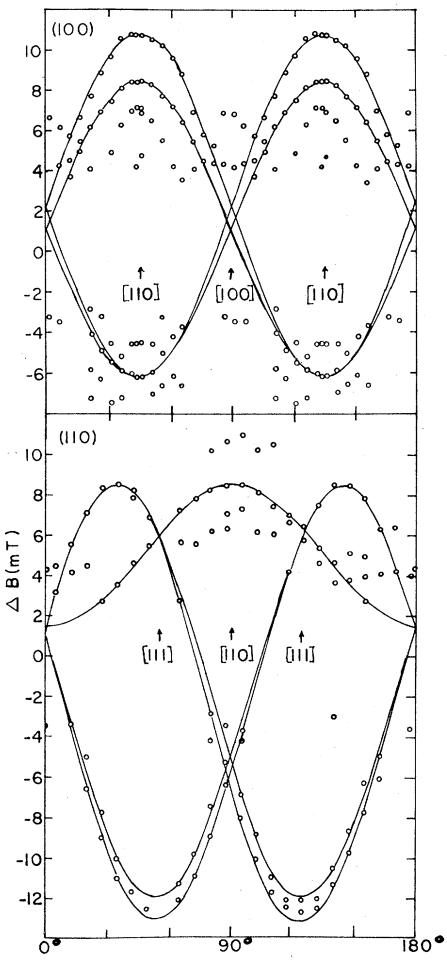

FIG. 2. Plot of line shifts vs angle between the [100] axis and the magnetic field for rotations in the (100) and (110) planes for $CaF_2(DyF_3)$.

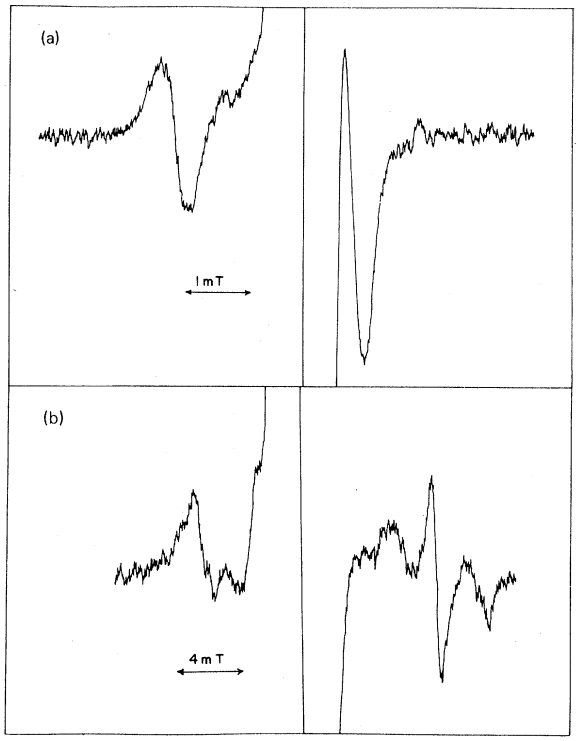

FIG. 3. (a) Spectrum for $CaF_2(NdF_3)$ with magnetic field along the [111] crystal axis at 46.6 MHz. (b) Spectrum for $CaF_2(DyF_3)$ with magnetic field along the [110] axis at 46.6 MHz.

III. RESULTS

A. Fluoride ions with one nearest neighbor

Spectra were recorded at 5° intervals through a 180° arc at 46.6 MHz for rotations of the magnetic field in the (100) and (110) crystal planes. Spectra were also recorded at 10° intervals in the (110) plane at 84.67 MHz for CaF_2 crystals containing 1% NdF_3 and EuF_3. All spectra were dominated by a strong central line (due to fluoride ions far from the rare earth ions) which was used as an internal reference for measuring the shift ΔB.

The most intense satellite resonances are due to lattice fluoride ions having one rare earth ion in the closest cation sites. These lines were identified and the shifts plotted as a function of angle for both the (100) and (110) rotational planes and were least squares fitted to the function.

$$\Delta B/B_0 = A\cos^2(\omega - \omega_{\max}) + B\,, \tag{4}$$

where A, B, and $\omega_{\max}$ (the angle where the shift maximizes) are constants. Typical plots in the (110) plane are shown in Figs. 1 and 2 for crystals doped with NdF_3 and DyF_3. Some typical spectra are given in Fig. 3. When the magnetic field is along the [111] axis one of these resonances is downfield and well separated from the rest of the spectrum. Intensity comparisons of this resonance line with the total ^{19}F intensity show that the ratio of F^- ions giving rise to this line to rare earth ions in the crystal is $\sim 2 \pm 1$.

NdF_3-, EuF_3-, and TmF_3-doped crystals all showed one set of resonance lines allowing a direct calculation of a_s and $a_p + a_m$ in Eq. (1) for these lines. For DyF_3- and HoF_3-doped crystals the lines became split indicating that the metal-ion–fluoride-ion direction vector is not exactly along the [111] cubic axis and/or there is present another rare-earth ion at a next-nearest-neighbor cation site. This distortion is presumably also

TABLE I. NMR-shift parameters for a lattice F^- in CaF_2 with one nearest-neighbor rare-earth ion.

Ion	$10^3 a_s$	$10^3(a_p + a_m)$	$10^3 a_m$(calc.) [a]	$[10^3 a_s^P]$ [b]	$[10^3 a_p^P]$ [b]	Ref.
Nd^{3+}	−0.03 ± 0.05	0.86 ± 0.02	0.70	0.14	0.08	c
Eu^{3+}	−0.21 ± 0.03	0.42 ± 0.03	0.62	−0.30	−0.18	c
Dy^{3+}	−1.23 ± 0.10	6.02 ± 0.10	6.49	−0.80	−0.47	c
Ho^{3+}	−0.93 ± 0.10	6.39 ± 0.10	6.44	−0.64	−0.38	c
Er^{3+}	−1.05 ± 0.07	5.41 ± 0.04	5.26	−0.43	−0.26	d
Tm^{3+}	−0.73 ± 0.04	3.42 ± 0.03	3.27	−0.23	−0.14	c
Yb^{3+}	−0.32 ± 0.08	1.17 ± 0.04	1.18	−0.07	−0.04	d

[a] Calculated from Eqs. (2) and (3) using $R = 235$ pm for Nd^{3+} and Eu^{3+} and $R = 230$ pm for the others. Equation (3) is not applicable for Eu^{3+} and an effective magnetic moment of 3.4 Bohr magnetons was used to calculate χ in Eq. (2).

[b] Calculated from Eqs. (5) and (6) using $K_{\parallel} = 3.60$ MHz and $K_{\perp} = 0.93$ MHz. These equations are not applicable to Eu^{3+} for which the calculations given in Ref. 18 were used.

[c] This work.

[d] Reference 2.

present for the other dopants but it is the larger shifts present for Dy^{3+} and Ho^{3+} that make it visible. Similar splittings were observed[2] for ErF_3-doped crystals. In calculating a_s and $a_p + a_m$ for DyF_3- and HoF_3-doped crystals, an average of these lines was taken at the critical directions of [111], [110], and [100].

Values of a_s and $a_p + a_m$ for all the crystals studied, so far, are given in Table I. Also given in Table I are calculated values of a_m using Eqs. (2) and (3). Since R is unknown in these systems we have chosen it to be 235 pm for Nd^{3+} and Eu^{3+} which is between the Ca^{2+}-F^- distance of 237 pm and the sum of ionic radii which is 230–232 pm. For the ions in the second half of the rare-earth series, ionic radii give $R < 220$ pm which is unlikely in CaF_2 so a small contraction was assumed and R was chosen to be 230 pm. Equation (3) is not applicable for Eu^{3+} which has a ground state of $J = 0$ plus excited states that are thermally populated at room temperatures. Measurements and theoretical calculations give an effective magnetic movement for Eu^{3+} of 3.4 Bohr magnetons at room temperature and this was used to obtain χ in Eq. (2).

A comparison of $a_p + a_m$ from experiment and the calculated value of a_m show reasonable agreement for Dy^{3+}, Ho^{3+}, Er^{3+}, Tm^{3+}, and Yb^{3+} considering the uncertainties in R. The differences for Nd^{3+} and Eu^{3+} are too large to be blamed on uncertainties in R and must be due to a_p having a significant magnitude compared to a_m. The difference for Eu^{3+} is particularly large. Explanations for this will be advanced in the discussion section.

B. Other resonances

In Figs. 1 and 2 other resonances can be seen that do not belong to fluoride ions having only one nearest-neighbor rare-earth ion. Resonances of this type were found in all systems studied. Unfortunately, most of these resonances could not be followed over a large enough range of angles to characterize their orientational behavior in a definitive fashion. These resonances were most often found when the magnetic field was close to either the [110] or [100] axes. Shifts for extra resonances along these two axes are given in Table II. In some instances the relative intensity of these resonances relative to the total ^{19}F intensity was measured and is also reported in Table II in terms of relative concentration of F^- ion to rare-earth ion concentration. The possible assignments for these resonances is advanced in Sec. IV B.

TABLE II. Shifts of resonance lines that cannot be assigned to lattice fluorides having one nearest-neighbor rare-earth ion.

Ion	$10^3(\Delta B/B_0)$ [100]	$10^3(\Delta B/B_0)$ [110]
Nd^{3+}	+1.66 ± 0.06 (1.0) [a]	+1.53 ± 0.05 (1.3) [a]
	−1.14 ± 0.06	−1.33 ± 0.04
Eu^{3+}	+0.92 ± 0.05	
Dy^{3+}	+3.70 ± 0.05 (0.4) [a]	+9.28 ± 0.10 (~1) [a]
	−2.99 ± 0.05	+5.67 ± 0.30
		−5.27 ± 0.10
Ho^{3+}	+2.84 ± 0.10	+8.38 ± 0.20
	−1.38 ± 0.10	+6.12 ± 0.10
	−2.75 ± 0.10	
Tm^{3+}	+4.92 ± 0.50 (0.6) [a]	+5.57 ± 0.20
	+4.34 ± 0.08 (0.5) [a]	+2.67 ± 0.30
	−1.51 ± 0.05	

[a] Ratio of F^- ions giving resonance to rare-earth ions in the crystal as estimated from NMR intensities, assuming nominal concentration of dopant ions to be correct. Except for the [110] line for Dy^{3+} the error in these ratios is ± (0.2–0.3).

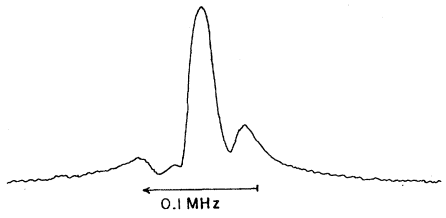

FIG. 4. Spectrum for $CaF_2(EuF_3)$ at 84.67 MHz with magnetic field along the [111] crystal axis.

C. T_1 measurements

The satellite lines could not be resolved adequately at 46.6 MHz for EuF_3 in CaF_2. They could, however, be resolved at 84.67 MHz using our FT high-power spectrometer. In this case, the bulk of the center line was removed by applying an 180° pulse and then waiting a time sufficient for M_z of the main central line to become zero before applying a measure pulse. A typical spectrum is given in Fig. 4 for the magnetic field along the [111] axis for 1 mol% EuF_3 in CaF_2. In doing a rotational study it was necessary to determine T_1 for the bulk fluoride ions at each orientation of the magnetic field. Plots of room-temperature values for T_1 for the magnetic field in a (110) plane were determined for CaF_2 containing 1 mol% EuF_3 and 1 mol% NdF_3 and these are plotted in Fig. 5. The values of T_1 changed markedly with orientation (nearly an order of magnitude for NdF_3) with the largest values for the [111] axis and shortest for the [100] axis.

IV. DISCUSSION

A. Fluoride ions with one nearest neighbor

In Table I it will be noted that experimental values of $a_p + a_m$ are close to the values of a_m calculated from Eq. (2) and (3) for all ions except Nd^{3+}

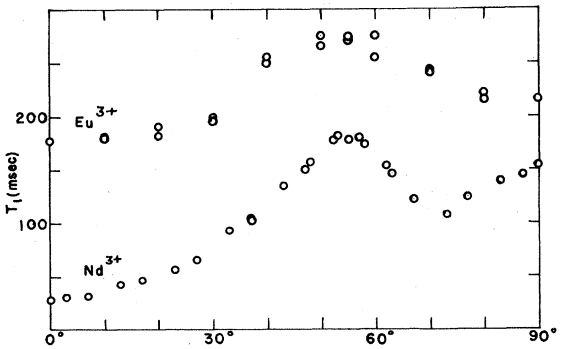

FIG. 5. T_1 vs angle between [100] axis and magnetic field for rotation in the (110) plane for 1% crystals of $CaF_2(NdF_3)$ and $CaF_2(EuF_3)$.

and Eu^{3+}. The small differences for all but Nd^{3+} and Eu^{3+} can easily be removed by small adjustments in the assumed values of R, but this cannot be done for Nd^{3+} and Eu^{3+} because the R values needed would be unreasonable. Therefore, for at least these two ions, a_p cannot be neglected.

Two mechanisms have been proposed in the literature for both a_s and a_p. The polarization mechanism was first proposed by Watson and Freeman.[15] In this mechanism electron spin is transferred to $2s$ and $2p$ orbitals of F^- by overlap interaction with $5s$ and $5p$ orbitals of the rare-earth ion. The spin in the $5s$ and $5p$ orbital have been polarized by an exchange interaction with the inner $4f$ unpaired electrons. Watson and Freeman[15] showed that the electrons in the outer regions of the $5s$ and $5p$ orbitals are polarized with spin opposite to that of the inner $4f$ electrons so that this mechanism leads to unpaired spin in the F^- orbitals of opposite sign to that of the $4f$ electrons. Although it is difficult to do direct calculations for this mechanism, the values of a_p and a_s due to this mechanism can be estimated using the following equations[13]:

$$a_s^P = -\frac{g_J(g_J-1)\mu_B J(J+1)}{9kTg_N\mu_N}(K_{\parallel}+2K_{\perp}) , \tag{5}$$

$$a_p^P = -\frac{g_J(g_J-1)\mu_B J(J+1)}{9kTg_N\mu_N}(K_{\parallel}-K_{\perp}) , \tag{6}$$

where $K_{\parallel}$ and $K_{\perp}$ are proportionality constants relating the contribution of this mechanism to the ^{19}F hyperfine interaction with the matrix element $\langle S\rangle$. $K_{\parallel}$ and $K_{\perp}$ have been determined[15-17] from ENDOR studies of Gd^{3+} in CaF_2 to be 3.60 and 0.93 MHz, respectively. Using these values a_s^P and a_p^P were calculated from Eqs. (5) and (6) and are given in Table I. Equations (5) and (6) were derived assuming excited states with different J values are much higher in energy than kT. This assumption is not true for Eu^{3+} for which $J=0$ in the ground state. For Eu^{3+} the values of a_s^P and a_p^P in Table I were calculated using a calculation of $\langle \bar{S}\rangle$ over all excited states performed by Golding and Halton.[18]

It is seen in Table I that a_s and $a_p + a_m$ are fairly well accounted for by the polarization mechanism in the case of Eu^{3+} and Nd^{3+}, although the a_s^P value is significantly different from experiment for Nd^{3+}. In the case of rare-earth ions in the second half of the rare-earth series, a_s^P is of the correct sign but significantly smaller in magnitude than the experimental a_s value. Also $(a_m + a_p^P)$ is less in agreement with $(a_p + a_m)$ than a_m alone. Theoretical calculations[19] of the covalent contributions a_s^C and a_p^C for Pr^{3+}, Nd^{3+}, Tb^{3+}, Ho^{3+}, Er^{3+}, Tm^{3+}, and Yb^{3+} show that a_s^C is negative and a_p^C is positive for all

these ions. Thus, in the second half of the rare-earth series a_p^C and a_p^P tend to cancel each other out making $a_p \sim 0$. a_s^C and a_s^P are of the same sign in this half of the series, however, giving rise to the sizable negative values of a_s found experimentally. For Nd^{3+} the reverse is true giving rise to a negligible a_s but a sizeable positive a_p term. No covalent calculation has been done for the special case of Eu^{3+}, but our experimental results suggest a_s^C and a_p^C are negligible for this ion.

B. Other resonances

In an earlier study[2] on YbF_3 in CaF_2 a series of resonances were found which could be identified as a lattice fluoride having two nearest-neighbor rare-earth ions. The two additional resonances in the [110] direction for Nd^{3+} in Table II are undoubtedly the same type. For this sytem there will be a line in the [110] direction with a large upfield shift given by

$$-a_s + 2(a_m + a_p)\,, \tag{7}$$

and a second line with a large downfield shift given by

$$-a_s - 2(a_m + a_p)(3\sin^2\beta - 1)\,. \tag{8}$$

The angle β is the angle between the [100] axis in the plane of the fluoride ion plus its two nearest-neighbor rare-earth ions and the vector between the fluoride ion and one of the rare-earth ions. The value of a_s is most likely somewhere between 0 and -10^{-4} which gives values of $a_m + a_p$ between 0.77×10^{-3} and 0.72×10^{-3}. The value of β lies between 52.1° and 54.7°. For an undistorted cubic lattice $\beta = 54.7°$ and $a_m + a_p$ would be similar to the value of 0.86×10^{-3} found for the lattice fluoride with one nearest neighbor. It seems clear from this that indeed the two extra resonances in the [110] direction arise from the same clustering found for YbF_3 in CaF_2. The distance between the fluoride ion and the rare-earth ion is longer for the lattice fluoride ion with two nearest neighbors than for the ion with only one nearest neighbor.

The two extra resonances observed in the [100] direction are not from the system discussed above. The line at $+1.66\times10^{-3}$ is probably the same as one observed[2] in the $CaF_2(ErF_3)$ system which was attributed to an interstitial fluoride with two nearest-neighbor rare-earth ions.

For $CaF_2(DyF_3)$ there are two resonances observed upfield in the [110] direction about the resonance attributed to a lattice fluoride with one rare-earth neighbor. They are of comparable intensity to that of the lattice fluoride resonance as can be seen in Fig. 3. Similar spectra were observed for crystals doped with Ho^{3+} and Tm^{3+}. As can be seen in Fig. 2 the upper line at [110] could be followed well enough in the (100) plane rotation to assign the line at -5.27×10^{-3} in the [110] direction to the same fluorides. Since the system giving rise to this resonance does not appear to give any lines with a large downfield resonance near the [111] orientation, it cannot be a fluoride with one rare-earth neighbor. If we assume it to be a lattice fluoride with two rare-earth ion neighbors, *and further that the* [100] *line at* -2.99×10^{-3} *comes from the same system,* we get $a_s = 0.34\times10^{-3}$, $(a_m + a_p) = 4.47\times10^{-3}$, and $\beta = 47.4°$. For $a_s = -1.0\times10^{-3}$, $a_m + a_p$ will equal 4.14×10^{-3} and $\beta = 49.9°$. Thus if this assignment were correct we would have $a_m + a_p$ considerably less than the value of 6.49×10^{-3} for a lattice fluoride with one rare-earth ion neighbor. Also the value of β is considerably below the expected cubic value. Similar behavior is found for the same resonances observed in Ho^{3+} and Tm^{3+} systems.

For the $CaF_2(YbF_3)$ system studied earlier, it was found that for the lattice fluoride with two rare-earth ion neighbors, the value of $a_m + a_p$ was greater than that of a fluoride with one neighbor and β was 63.5°, which is considerably greater than that of a purely cubic system. It is possible to consider the above assignment of the lines in $CaF_2(DyF_3)$ to a lattice fluoride with two nearest rare-earth ion neighbors as correct and still reconcile the different values of β and $a_m + a_p$ found for different rare-earth ions by noting that both values of β have been found[16] in an analysis of ENDOR[20] and NMR[3] of lattice fluorides next to a single Yb^{3+} ion with an interstitial fluoride in the closest interstitial site. In this case $\beta = 62°$ for fluoride ions between the rare-earth ion and the interstitial fluoride and $\beta = 51°$ for fluorides on the opposite side.

We propose that one consistent way to explain the extra resonances with large shifts in the [110] direction is to assume they come from lattice fluorides with two nearest-neighbor rare-earth ions but that these rare-earth ions are not located in the cubic center. Rather they are both displaced in the same direction along a [100] axis presumably towards neighboring interstitial fluoride ions. This distortion would produce two different types of lattice fluorides with different values of β and R. To get a rough idea if this model will quantitatively predict what we observe, we can assume that the cubic array of lattice fluorides is rigid and that the distortion of rare-earth ion occurs only to the extent allowed by the sum of ionic radii for the rare-earth and fluoride

ions. For Yb^{3+} the sum of radii is 214 pm which predicts the two lattice fluorides between the Yb^{3+} ions to have values of $\beta = 64.7°$, $a_m = 1.46 \times 10^{-3}$ and $\beta = 46.7°$, $a_m = 0.76 \times 10^{-3}$. The first set of values is close to the experimental values of $\beta = 63.5°$, $a_m + a_p = 1.34 \times 10^{-3}$. The other set of lines predicted by the second set of values would be difficult to see because they would fall nearly on top of the cubic lines for a lattice fluoride with one nearest neighbor, at least for the [110] direction which generally gives the largest shifts. For Dy^{3+} the sum of radii is 221 pm and would predict $\beta = 61.1°$, $a_m = 7.32 \times 10^{-3}$ and $\beta = 49.2°$, $a_m = 4.73 \times 10^{-3}$. The second set of values are close to those observed experimentally. The other set of values would predict lines of large and easily detectable shifts but it may be that these lines are too broad to detect easily due to very short T_1 values. This is reasonable because the observed lines are considerably broadened compared to those of fluoride ions with one rare-earth neighbor so that it is reasonable to suppose that the other set of fluorides with their smaller value of R would have much shorter T_1's than the observed sets. The reason the resonances from the set with the smaller R value could be seen in Yb^{3+} and not for Dy^{3+}, Ho^{3+}, and Tm^{3+} is due to the much smaller magnetic moment for Yb^{3+} compared to the other ions.

For Nd^{3+} we again have a small magnetic moment comparable to Yb^{3+}. The sum of radii for Nd^{3+} is 232 pm and predicts the values of $\beta = 56.5°$, $a_m = 0.73 \times 10^{-3}$ and $\beta = 53.0°$, $a_m = 0.64 \times 10^{-3}$. These values are so close that only one line would be detected predicting $\beta = 54.7°$ and $a_m = 0.69 \times 10^{-3}$. These are close to the values found experimentally.

Although it is highly speculative it is surprising how well this model accounts for what is observed across the rare-earth series. There are still lines that are unassigned. Most of those observed in the [100] direction are undoubtedly interstitial fluorides with one or more nearest-neighbor rare-earth ions. The upfield line in the [110] direction of smaller shift for Dy^{3+}, Ho^{3+}, and Tm^{3+} could be a lattice fluoride with one nearby rare-earth ion at a larger distance of 250–270 pm but this is very uncertain.

If this interpretation is correct it could be deduced that the clusters giving rise to these extra resonances have a sheet of rare-earth ions in a (100) plane with an adjacent plane containing a sheet of interstitial fluorides. The resonances from the lattice fluorides with one nearest neighbor could then come from cubic sites. The intensities would require about half the rare-earth ions to be in cubic sites and half in such clusters. It may be that other geometrical arrangements would equally well explain what we have observed, so we cannot put this forth more strongly than as a suggestion.

C. T_1 measurements

A large number of studies of T_1 or $T_{1\rho}$ for ^{19}F in alkaline-earth fluorides doped with various rare-earth ions have appeared, but only a few[21–25] have reported variations with orientation and mostly at temperatures well below room temperature. As we shall see, the main reason for not detecting such dramatic changes at room temperature is the frequency used for measurement. Although a few studies of T_1 at 30 MHz have been reported, most studies have been done at frequencies below 15 MHz.

The theory of T_1 in diamagnetic systems having paramagnetic impurities was first presented by Bloembergen[26] who postulated that the bulk magnetization relaxed by diffusion towards a paramagnetic site via the nuclear dipolar relaxation and then was equilibrated with the lattice by the interaction between the paramagnetic ion and the nearby lattice nuclei. Two limiting cases were distinguished: diffusion-limited relaxation and rapid diffusion. In the first case the slow step is the rate of diffusion of the magnetization to the paramagnetic site. In the second case the rate is determined by the rate of equilibration of neighboring nuclei with the lattice via their interaction with the paramagnetic ion. Khutsishvili[27] and de Gennes[28] found equations for T_1 for the case of slow diffusion while Blumberg[29] obtained the equation for the case of rapid diffusion. Rohrschach[30] derived an equation for the region between the two limiting cases giving the earlier results as proper limits. Lowe and Tse[31] extended Rohrschach's theory to systems of higher concentration where there can be more than one paramagnetic site and also developed the theory for $T_{1\rho}$, the relaxation time in the rotating frame. Important in all these theories is the concept of a "barrier radius" inside of which spin diffusion cannot occur because the local field of the paramagnetic ion has shifted the resonance of nuclei inside the barrier too far away from the other nuclei so that the spin-flip mechanism, which requires both nuclei to have the same resonance frequency is quenched. We shall show that the large variation observed for T_1 in Nd^{3+}-doped crystals is due to large changes in this "barrier radius" with orientation.

The equation obtained by Rohrschach for T_1 is

$$T_1 = (\tfrac{8}{3}\pi N D \beta_1)^{-1}[I_{-3/4}(\delta)/I_{3/4}(\delta)], \tag{9}$$

$$\delta = \beta_1^2/2b^2, \tag{10}$$

$$\beta_1 = (\overline{C}/D)^{1/4}, \tag{11}$$

where b is the "barrier radius," and N is the number of paramagnetic sites per unit volume. D is the diffusion coefficient for spin diffusion and $I_m(x)$

is the modified Bessel function. $\overline{C}$ is the parameter relating the rate of equilibration of nuclei through the paramagnetic ion to the distance between the nucleus and the ion

$$[\tau(r)]^{-1} = \overline{C}/r^6 . \tag{12}$$

A calculation of $\overline{C}$ requires a knowledge of the correlation time for the interaction. We can estimate it, however, from measurements of T_1 made on a single crystal of NdF_3. When the magnetic field is along the c axis of NdF_3, three resonances are observed from fluorides in three nonequivalent sites in the crystal. We have measured T_1 for these three resonances at room temperature and found $T_1 = 372$ μsec for the most abundant fluorides in general sites and $T_1 = 347$ and 117 μsec for the two special sites. If we take the average value of these three numbers for $[\tau(r)]^{-1}$ in Eq. (12) and $r = 230$ pm, we obtain an estimated value of $\overline{C} = 6.97 \times 10^{-55}$ m^{6}sec^{-1}. D has been estimated[32] to be 13.0×10^{-17} m^{2}sec^{-1}. This gives then a value of $\beta_1 = 271$ pm.

For the [100] orientation of the magnetic field we can see from Fig. 1 that the nearest fluoride ions to the rare-earth ion have the same resonance frequency as the bulk fluorides so that for this orientation $b \cong 232$ pm and $\delta = 0.68$ which means the system is in the transition region between the fast and slow diffusion limits. Using Fig. 1 from Rohrschach[30] and Eq. (9) this value of δ gives

$$T_1 = 25 \text{ msec},$$

which is surprisingly close to the value of 29.4 msec found experimentally. For the [111] orientation all the resonances from the nearest fluoride ion from both the fluorides with one nearest neighbor and the clusters are well shifted away from the bulk resonances and b must increase to the distance from the next-nearest neighbor which is about 454 pm. This value of b gives $\delta = 0.18$ which in turn gives

$$T_1 = 170 \text{ msec},$$

which is again surprisingly close to the value of 177.8 msec found experimentally.

Thus we see that present theories will fully account for the large variation in T_1 with orientation that was observed in this work. The reason earlier studies failed to see this large variation is due to the low fields they used in their studies. In this case the resonances of the closest fluorides overlap significantly that of the bulk fluorides at all orientations such that b remains constant at ~232 pm and the system remains close to the rapid diffusion limit in all orientations. At significantly lower temperatures the shifts become much greater and the orientational dependence can and has been detected. For a spectrometer operating at 10 MHz the temperature will have to be ~35 °K to see the same variation seen by us at room temperature in $CaF_2(NdF_2)$.

V. CONCLUSIONS

We have found that the significant clustering reported by us[2] for ErF_3 and YbF_3 doped into CaF_2 at concentrations $\gtrsim 0.5$ mol% is exhibited by NdF_3, EuF_3, HoF_3, and TmF_3 also and must therefore be common for all rare-earth ions. Further, there are systematic features in the NMR of fluoride ions in these clusters that lead to interesting speculations as to the nature of these clusters. We have also found that the conclusions[19] we had reached on spin transfer mechanism for pure rare-earth fluorides hold also for those ions doped into CaF_2; namely, that the polarization mechanism predominates in the first half of the rare earth series but the covalent mechanism is not negligible and becomes predominant in the second half of the rare-earth series. Finally we have found a large anisotropy in T_1 for the bulk fluoride resonances which is quantitatively accounted for by theories presently in the literature.

ACKNOWLEDGMENT

This work was supported by the Natural Science and Engineering Research Council of Canada.

*Present address: Building Materials Technology, Research Centre, Domtar Inc., Senneville, Quebec, H9X 3L7, Canada.

†Author to whom requests for reprints should be addressed.

[1] See, *Crystals with the Fluorite Structure*, edited by W. Hayes (Clarendon, Oxford, 1974).

[2] R. J. Booth, M. R. Mustafa, and B. R. McGarvey, Phys. Rev. B 17, 4150 (1978).

[3] J. P. Wolfe and R. S. Markiewzc, Phys. Rev. Lett. 30, 1105 (1973).

[4] E. Banks, M. Greenblatt, and B. R. McGarvey, J. Chem. Phys. 58, 4787 (1973).

[5] M. R. Mustafa, W. E. Jones, B. R. McGarvey, M. Greenblatt, and E. Banks, J. Chem. Phys. 62, 2700 (1975).

[6] D. R. Tallant, D. S. Moore, and J. C. Wright, J. Chem. Phys. 67, 2897 (1977).

[7] N. E. Kask and L. A. Korvienko, Fiz. Tverd. Tela (Leningrad) 9, 2291 (1967) [Sov. Phys.–Solid State 9, 1795 (1968)].

[8] J. M. Baker and D. Marsh, Phys. Lett. A 35, 415 (1971).

[9] A. K. Cheetham, B. E. F. Fender, D. Steele, R. J. M. Taylor, and B. T. M. Willis, Solid State Commun. 8,

171 (1970).
[10]A. K. Cheetham, B. E. F. Fender, and M. J. Cooper, J. Phys. C 4, 3107 (1971).
[11]C. R. A. Catlow, J. Phys. C 6, 64 (1973); 9, 1859 (1976).
[12]P. P. Yaney, D. M. Schaeffer, and J. L. Wolf, Phys. Rev. B 11, 2460 (1975).
[13]B. R. McGarvey, J. Chem. Phys. 65, 962 (1976).
[14]M. R. Mustafa, B. R. McGarvey and E. Banks, J. Magn. Reson. 25, 341 (1977).
[15]R. E. Watson and A. J. Freeman, Phys. Rev. 106, 251 (1967).
[16]B. R. McGarvey, J. Chem. Phys. 65, 955 (1976).
[17]J. M. Baker, Proc. Phys. Soc. London 1, 1670 (1968).
[18]R. M. Golding and M. P. Halton, Aust. J. Chem. 25, 2577 (1972).
[19]A. Reuveni and B. R. McGarvey, J. Magn. Reson. 34, 181 (1979).
[20]J. M. Baker, E. R. Davies and J. P. Hurrell, Proc. R. Soc. London Ser. A 308, 403 (1968).
[21]D. Tse and I. T. Lowe, Phys. Rev. 166, 292 (1968).
[22]N. A. Lin and S. R. Hartmann, Phys. Rev. B 8, 4079 (1973).
[23]R. Burnett, Physica (Utrecht) 32, 433 (1966).
[24]J. R. Miller and P. P. Mahendroo, Phys. Rev. 174, 369 (1968).
[25]C. M. Verber, R. G. LeCander, and W. H. Jones, Jr. Phys. Rev. Lett. 20, 852 (1968).
[26]N. Bloembergen, Physica (Utrecht) 25, 386 (1949).
[27]G. R. Khutsishvili, Proc. Inst. Phys. Acad. Sci. Georgia (USSR) 4, 3 (1956).
[28]P. G. de Gennes, J. Phys. Chem. Solids 7, 345 (1958).
[29]W. E. Blumberg, Phys. Rev. 119, 79 (1960).
[30]H. E. Rohrschach, Jr. Physica (Utrecht) 30, 38 (1964).
[31]I. J. Lowe and D. Tse, Phys. Rev. 166, 279 (1968).
[32]L. J. Humphries and S. M. Day, Phys. Rev. B 12, 260 (1975).